

* This report summarises the outcomes from the UK NC3R's and POEM's Maths Study Group meeting, 8th –12th September 2014 in response to a problem entitled 'Improving the utility of *Drosophila melanogaster* for neurodegenerative disease research by modelling courtship behaviour patterns', presented by BB and CS.

Improving the utility of *Drosophila melanogaster* for neurodegenerative disease research by modelling courtship behaviour patterns

Birgit Brüggemeier¹, Christian Schusterreiter¹, Hania Pavlou¹, Neil Jenkins², Stephen Lynch³, Arianna Bianchi⁴, and Xiaohao Cai⁵

¹University of Oxford

²University of Warwick

³Manchester Metropolitan University

⁴Heriot-Watt University, Edinburgh

⁵University of Cambridge

July 6, 2015

Abstract

Courtship in *Drosophila* is used to screen genes linked to Parkinson Disease in humans [13]. Courtship has been shown to allow more precise identification of physiological impairments in Parkinson Disease models than other fly behaviours [13]. Precise identification of early stage impairments of neuronal tissue in flies may influence experimental design in studies using mammals, and thereby address the goals of 3Rs by refining animal studies and reducing the number of animals used in research. *Drosophila* courtship behaviour is mostly neglected in disease and drug screens in flies, apart from few exceptions [13]. One reason for neglecting courtship behaviour, despite its advantages to other behaviours, may be the complexity of courtship behaviour. We have developed three models of fly courtship to study potential mechanisms underlying this complex behaviour. We have found that dynamics of fly courtship behaviour can be modelled reasonably well as a Markovian stochastic process. A stochastic model can act as baseline assumption of behavioural patterns being random. Deviations from randomness may then be explained by sexual drive: The female influences courtship choices of the male by sexually motivating him, as Margaret Bastock suggested in her model of male courtship [4]. We apply Bastock's theory in two neuronal models, a Paseman-like model [21], and a Fitzhugh-Nagumo model [28, 29]. Our two neuronal models complement one another as the Paseman-model is analytically tractable and the Fitzhugh-Nagumo model can simulate neuronal spiking. We modelled sexual motivation as firing frequency of model neurons. Our preliminary results suggest that our neuronal models can simulate courtship dynamics. Our neuronal models are the first mathematical formulation of courtship behaviour in *Drosophila* and can act as baseline for detecting behavioural deviations, as neuronal drive is the currently accepted baseline model for explaining *Drosophila* courtship patterns. In following-up our work we currently develop techniques to compare baseline simulations, with real behaviour, which will simplify quantification and interpretation of behavioural deviations. We aim to disseminate our models and techniques as tools for studying disease models in courtship behaviour of *Drosophila melanogaster* to promote usage of courtship behaviour, as courtship demonstrates higher sensitivity and specificity in identifying early onset impairments in Parkinson Disease. This may help to design better experiments with mammals and therefore reduce the number of animals used in research. In addition our models are not restricted to pattern generation of courtship in flies, but can be applied to behavioral pattern generation in general. This includes motor actions like walking and chewing, which are impaired in humans suffering from a neurodegenerative disease as Parkinson.

1 Introduction to *Drosophila* Courtship

Innate courtship of the male fruit fly *Drosophila melanogaster* consists of a series of behaviours which alternate in a complex pattern [2]. The courtship ritual of the male fly consists of a series of behaviours as orientation towards the female, wing extension and copulation. Figure 1 depicts courtship as a series of successive behaviours.

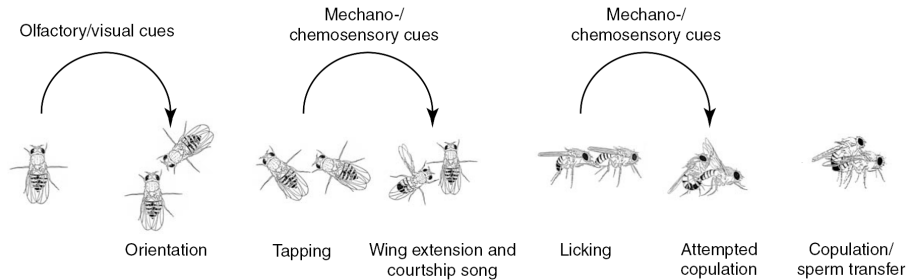


Figure 1: Courtship behaviours as presented by Billeter et al. [2].

However, transitions between courtship behaviours seem probabilistic as the male fly can switch from any courtship behaviour to any other courtship behaviour [3, 6, 8]. Figure 2 presents an ethogram of courtship behaviour taken from Cobb et al. [6]: boxes denote to different courtship behaviours, while arrows between boxes indicate the probability of a switch through the arrow's thickness.

In the 1950s, Margaret Bastock presented an idea to account for the problem of behavioural switches in innate fly courtship [4]. Her theory involves excitatory thresholds and varying excitation in the male fly. In the course of courtship male flies become increasingly sexually excited [4, 1, 17]. Courtship behaviours are assumed to be hierarchical in the level of excitation they require to be displayed [4]. Courtship is generated by one common network, with neuronal subsets sensitive to different excitatory frequencies [9]. The neural network determining courtship in the male fly consists of about 650 cells [9]. Through the use of genetic tools, it is possible to narrow down even smaller neuronal subsets which are responsible for specific courtship behaviours [10]. These neuronal subsets can be tested both for their necessity in generating a given behaviour (through neuronal deactivation) and their sufficiency in generating a behaviour (by artificial neuronal excitation). Thus *Drosophila* allows for a systematic study of behavioural choice.

2 Potential Impact on 3Rs and Human Healthcare

2.1 Relevance to Replacement, Reduction and Refinement of animal experiments

Promoting fly courtship as screening tool may refine experiments with mammalian laboratory animals, as fly courtship allows more precise identification of

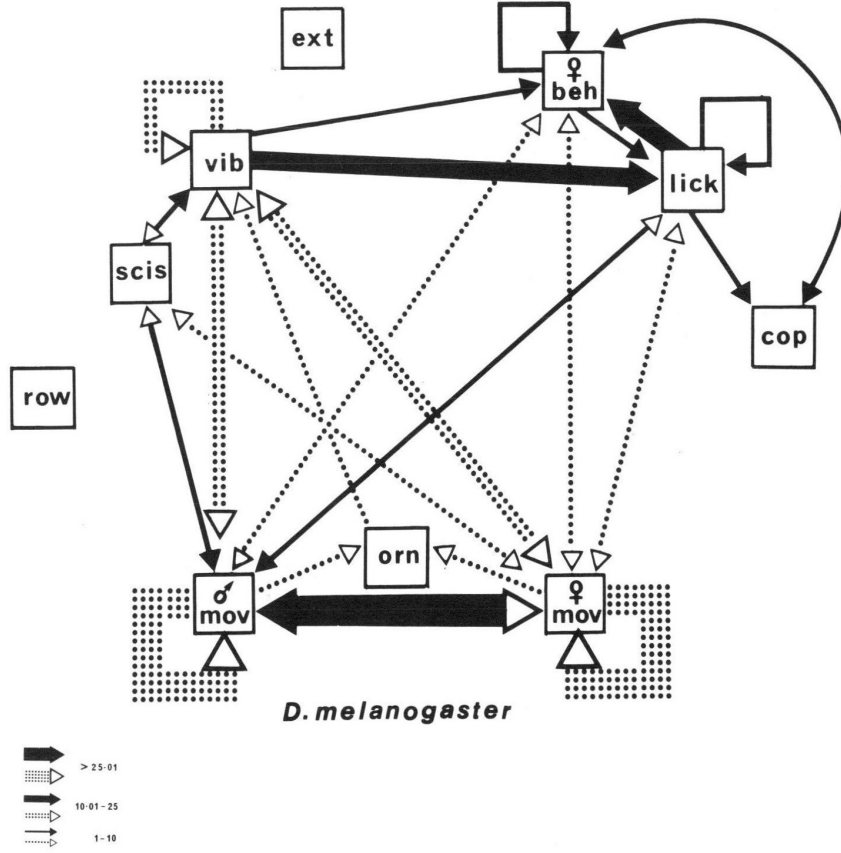


Figure 2: Ethogram of courtship behaviour for *Drosophila melanogaster*. The text in the graph’s boxes denotes to sub-behaviours of courtship: σ mov stands for male movement, orn stands for male orienting towards the female, φ mov stands for female movement, scis stands for wing scissoring, that is simultaneous extension of both wings, row stands for wing rowing, that is wing extension followed by immediate wing swing in, vib stands for wing vibration, ext stands for wing extension, lick stands for the male licking the female genitalia, φ beh stands for a class of behaviours shown by the female to express acceptance or rejection and cop stands for copulation. The thickness of arrows represents the frequency of transitions observed during courtship experiments. For this transition frequencies are grouped in three classes, which are given in the figures key: over 25 instances of a transition, 10 to 24 instances of a transition and transitions that occurred less than 10 times. Black arrows denote transitions significant at $P \leq 0.01$ in a stepwise search for identifying subsets of behaviours that significantly deviate from the assumption of quasi-random transitions. Accordingly, dotted arrows are not significant at $P \leq 0.01$. The ethogram is reprinted from Figure 5 of Cobb et al. [6].

physiological impairments in disease models than other fly behaviours that are more commonly used for disease screens [13]. When research in flies can show

that genes believed to trigger neurodegeneration in old animals only, actually affect young animals in clearly evident ways [13], this can affect how genes are believed to function and thus the design of follow-up experiments in mammals. For example Shaltiel-Karyo and colleagues show that Parkinson Disease is evident in young flies’ disfunctional courtship, but not in their climbing ability. The demonstration of early-onset PD impairments in flies courtship can be an argument for initiating PD studies in mammals earlier, while they suffer less from consequences of PD interventions, but already may show physiological and behavioural impairments.

We therefore wish to promote the use of courtship as sensitive behavioural measure in disease screens in the fly community. One problem for using fly courtship as a standard behavioural tool for quantifying disease related impairment is the complexity of courtship and the associated difficulty to define normal courtship. Modeling can help solving this problem by providing techniques and tools that define normal courtship on the basis of current theories of how *Drosophila* courtship patterns emerge. Currently courtship is quantified mainly with summary measures as the percentage of time spent courting (CI). CI is easy to quantify and comprises courtship to one index. This allows for large scale comparisons. However, simplifying courtship to one index omits differences in behavioural pattern. Courtship patterns are sensitive measures of the well-being of flies [4, 13]. The models and techniques we describe here can be a starting point for measuring behavioural patterns in courtship and in this way identifying otherwise overlooked impairments in disease screens.

Stochastic models of fly behaviour have been used as baseline model to detect subtle differences in behavioural patterns of different fly species [14]. Therefore stochastic models also may act as tools to screen for and detect subtle differences in courtship patterns of healthy and disease model flies. While stochastic models have been used as baseline models in *Drosophila* behaviour research before [14] fly behaviour has not yet been tested on fulfilling criteria of randomness like memorilessness. We therefore apply stochastic modelling to *Drosophila* courtship and demonstrate techniques to test for true randomness in behavioural data.

There are different ways to model *Drosophila* courtship behaviour. During the workshop we have pursued both probabilistic and deterministic modelling approaches, that can both act as baseline models to detect subtle differences in behavioural pattern. We chose our models to be informable with our behavioural data and to be in concordance with existing theories of courtship behaviour. Having models based on courtship behaviour, we can fit model parameters to observations of healthy and diseased flies’ courtship. We experimented with two deterministic models of neuronal activity, a Paseman-like model [21] and a Fitzhugh-Nagumo model [28, 29]. With them we started to test Margaret Bastocks hypothesis, which states that switches between courtship are due to hierarchical activity thresholds for successive courtship behaviours [4]. The two deterministic models we have studied have the advantage that they include a physiological mechanism. Each behaviour is seen as the result of neural activity, that triggers the behaviour when the activity or firing level is above a certain threshold. Although this kind of model includes parameters which are difficult to estimate, parameter estimation is possible through established statistical tools as Approximate Bayesian Computation [19, 20].

2.2 Relevance to Human Medicine and Healthcare

While we emphasise the *Drosophila* courtship in our report, our models are applicable for other behavioural patterns in other animals like Humans *Drosophila*. Potentially interesting candidates are walking and chewing, which are impaired in humans suffering from Parkinson Disease. Our models could act as baseline models for identifying deviations from normal patterns. For instance human walking could be video recorded and analysed on distance between footsteps, time till shifting weight from one foot to the other and general velocity. These parameters could then be put into either stochastic or deterministic models to simulate a baseline behavioural motif on the assumption that these parameters vary randomly (stochastic model) or depend on excitation (deterministic models). The baseline assumptions may then help to identify deviations.

3 Initial Questions and Objectives

At the beginning of the workshop we asked the following three questions:

1. Can we expand Birgit Brüggemeiers (BB) courtship song model to courtship as a whole?

BB has developed a simple model of *Drosophila* courtship song (unpublished). Song consists of two qualitatively different modes: sine and pulse song. BBs model resorts to Margaret Bastock's hypothesis of hierarchical excitation thresholds to explain why a fly chooses to sing sine respectively pulse song [4]. In courtship song the experimental data basis is sufficient to develop a simple model of courtship song [15, 16, 18]. During the workshop we have found, however, that the data basis for courtship as a whole is not sufficient to model courtship as a function of realistic physiological processes. Song choice restricts analysis to wing movement, while courtship analysis has to account for movement of various body parts. The interaction between various body parts and the underlying physiological mechanisms is yet subject to assumptions. We have started testing whether or not the simple hypothesis of hierarchical excitation thresholds can account for switches between courtship behaviours.

2. How can we mine for possible models in large amounts of behaviour data?

We have used stochastic Markov processes to mine for behavioral patterns in normal and mutant flies. For stochastic models behaviour mining is a straightforward, well-known process. However, it is still a challenge to show that stochastic models are applicable and to minimize potential assumptions that come with model choices. For the Markov property to hold we require the process to be memoryless, while this initially seems like a very strong assumption to make about the behaviour if it is indeed valid then the problem is mathematically far more approachable. To test the Markov property we needed to check whether the times spent in each state of courtship were distributed exponentially. Preliminary analysis indicated that the times did indeed seem to follow an exponential distribution. We have therefore shown that the underlying conditions for a Markov model being applicable are not just assumed to be true,

but are indeed supported by our data.

3. What are advantages and disadvantages of these models?

This will be discussed below in the presentation of the respective models. However we would like to emphasise here that a general benefit of our models is that they can be applied to various behavioural patterns in species ranging from flies to humans.

4 Mathematical Models

4.1 Probabilistic Model - Markov Process

In order to produce a model which was primarily data driven, we chose to implement a stochastic model. This approach allowed for a minimal assumption set and could have parameters which were found directly from the available data.

To begin constructing the stochastic model we first interrogate the existing data. In order to simplify the modelling we first checked whether the Markov property would hold for the system in question. The Markov property states that the next state of the system depends only on the current state and not on previous ones. This is a type of memoryless quality, however, it does not necessarily imply that the male fly has no memory, just that the decisions made only depend on the current state. The Markov property requires that the dwell times in each state (that is, the amount of time spent in a state before changing state) must follow an exponential distribution. Since we already have access to a large amount of data we were able to produce an empirical cumulative density function (CDF) and then check for an exponential distribution by plotting the logarithm of the (1-CDF) function of each of the categories of dwell data. We can see that these plots (Figure 3) appear to follow a straight line and we therefore conclude that the Markov property is a reasonable one to assume.

We can now begin to define a continuous time Markov process to model the system. We choose a continuous time model since the actions of the fly occur in continuous time, even though the measurements taken are from video frames and are therefore discretised. We first define the state space and jump rates of the process. We use a random walk process on a graph with four nodes because the data available was scored into four categories: No courtship, Following, Wing extension and Copulation (see Figure 4).

4.1.1 Model Definition

Let $(\eta_t)_{t \geq 0}$ be an asymmetric random walk on the graph Λ_N of N nodes. The state of the process at time t , which indicates which node the random walker occupies is denoted by $\eta_t \in N, F, S, C$. We denote the rate of jumping from state i to state j by $\omega_{i,j}$. We can therefore construct the jump matrix of the process according to the graph structure illustrated.

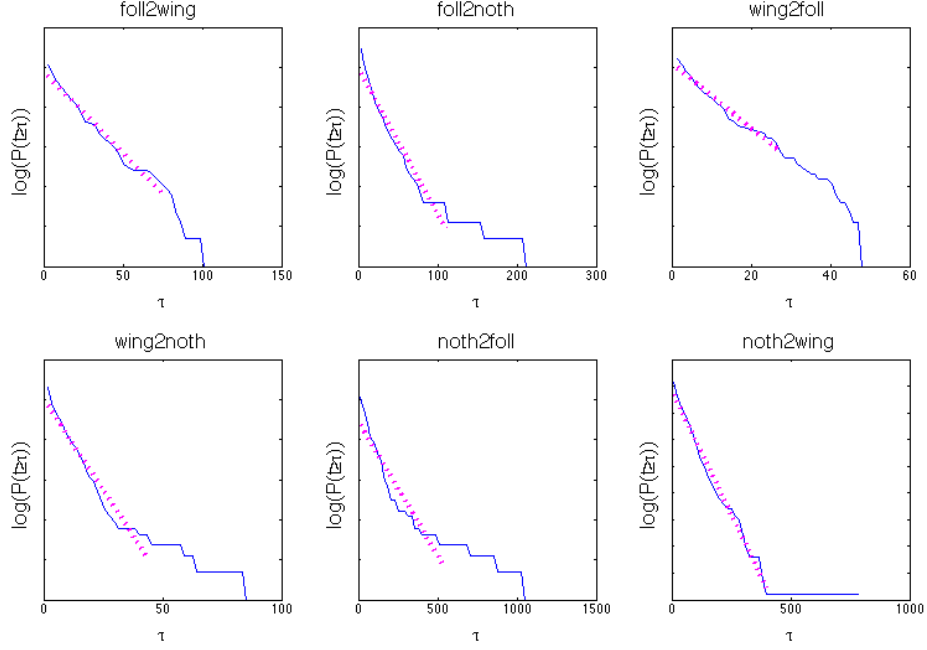


Figure 3: Logarithmic plots of the empirical 1-CDF for the observed data. The linearity of the plots near the Y-axis suggests that the Markov property is likely to be a resonable feature to assume in the model.

$$\mathbb{J} = \begin{pmatrix} \Omega & \omega_{F,N} & \omega_{W,N} & 0 \\ \omega_{N,F} & \Omega & \omega_{W,F} & 0 \\ \omega_{N,W} & \omega_{F,W} & \Omega & 0 \\ \omega_{N,C} & \omega_{F,C} & \omega_{W,C} & 0 \end{pmatrix},$$

where $\Omega = -(\omega_{F,N} + \omega_{F,W} + \omega_{F,C})$. From the jump matrix it is now possible to construct a master equation for the process to show how the probability density evolves across the state space in time.

$$\frac{d}{dt} \begin{pmatrix} \mathbb{P}(N) \\ \mathbb{P}(F) \\ \mathbb{P}(W) \\ \mathbb{P}(C) \end{pmatrix} = \mathbb{J} \times \begin{pmatrix} \mathbb{P}(N) \\ \mathbb{P}(F) \\ \mathbb{P}(W) \\ \mathbb{P}(C) \end{pmatrix}.$$

Since this process has an absorbing state, i.e. once the process enters the copulation state it cannot leave, the stationary solution to the master equation is trivial and corresponds to all of the probability density being in the copulation state:

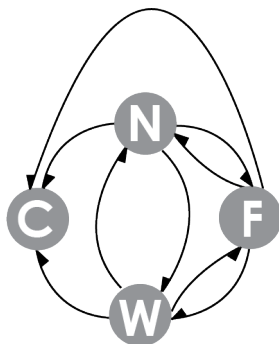


Figure 4: A schematic of the state space of the Markov process. N denotes No courtship, F is Following, W is Wing extension and C represents Copulation. The connections in the schematic are based on behavioural observations: *Drosophila melanogaster* can switch from any behaviour to any other behaviour represented in the schematic – except for copulation. Copulation terminated courtship behaviour. Therefore the schematic shows transitions to copulation only and none from copulation.

$$\frac{d}{dt} \begin{pmatrix} \mathbb{P}(N) \\ \mathbb{P}(F) \\ \mathbb{P}(W) \\ \mathbb{P}(C) \end{pmatrix} = \begin{pmatrix} 0 \\ 0 \\ 0 \\ 1 \end{pmatrix}.$$

4.1.2 Simulations

In order to obtain a preliminary picture of whether the model outlined above can actually generate similar behaviour to that observed in actual courtship experiments, we ran computer simulations of the process. This involved modelling a single object which could be in one of four states, corresponding to the states in the model above. Since we are assuming that the model is Markovian the wait times in any given state are distributed exponentially,

$$t \sim \lambda e^{-\lambda t},$$

with $\frac{1}{\lambda}$ being the mean wait time in the state. It is then possible to draw a (pseudo) random time from this distribution using the inverse CDF method such that

$$t = -\frac{\ln(x)}{\lambda},$$

where $x \in (0, 1)$ is a pseudorandom number drawn from a uniform distribution on the unit interval.

This is all that is required to simulate the switching between states that we wish to model. We then ran this simulation using mean wait time which were calculated from the experimental data which we had. This could then be used to generate an ethogram in a similar fashion to those shown in the data.

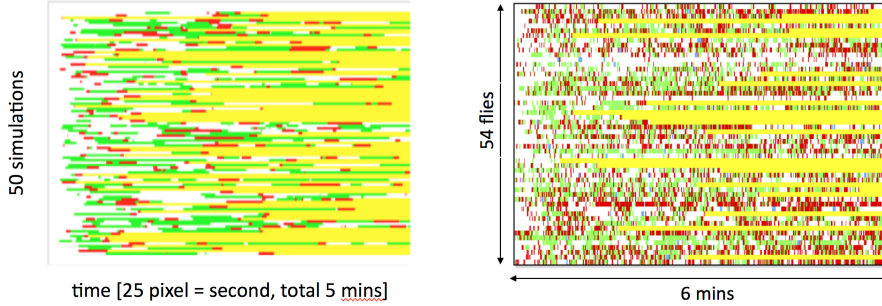


Figure 5: Left: An ethogram of behaviours exhibited over time generated from the simple random walk model. Right: An example of a real ethogram produced from analysing courtship videos. The colour-bars represent different behaviours. White stands for no courtship behaviour is shown, green for following behaviour, red for courtship singing and yellow for copulation.

The ethograms generated (Figure 5) appear to follow similar patterns to the real data obtained from courtship videos. In order to quantify the closeness of the generated data to that obtained from experiment we need to define a metric. This will allow us to determine the optimum parameters to generate data which is closest to that observed. This will hopefully also show the validity of the assumptions in the model if the fitted rates are close to those which are calculated from the data.

This model can be expanded by applying it to other graph structures for the behavioural states. This could allow for the inclusion of a richer set of states or potentially applications to other behaviours than courtship.

4.2 Neuronal Models

When modelling the courtship patterns of *Drosophila melanogaster*, it has been observed that certain neurons fire during the differing stages of courtship. We decided to focus upon a simple model of four neuron clusters, namely: Processing unit (P), which corresponds to no behaviour; Following cluster (F), which in fact comprises several neuron types activated while following behaviour is displayed; Wing vibration cluster (W), more precisely defined as mesothoracic cluster; and finally Copulation cluster (C), located in the abdomen. As a simple starting point, we are going to consider these four neuronal clusters interconnected with differently weighted excitatory and inhibitory connections between them. For simplicity, we assume that the neurons in one cluster fire at the same time, so that we can model each cluster as a single neuron. There are biological reasons to consider each cluster modelled as one neuron. Each of the behaviours can be linked to a group of neurons which share a specific feature, for example an active gene sequence. When these neurons are activated *at the same time*, the behaviour is displayed. Hence we can justify model a set of neurons with one neuron both with those neurons all sharing one biological feature (active gene sequence) and with observing behaviour when all neurons in that given set are activated at the same time.

In the following, two different models are introduced to describe the intercon-

nections amongst these neuronal clusters: a simple difference equations system and a Fitzhugh-Nagumo one. If the models outputs fit well the observed behavioural data, they will potentially have a great value in identifying impaired neural connections in neurodegenerative cases.

4.2.1 Pasemann-Like Model

In the 1990s, Pasemann proposed a simple model to describe interactions between neurons [21, 22]. Here the dynamics of neuronal interactions are described by discrete-time difference equations. To every “unit” (neuron) i corresponds one equation describing its *activation* a_i which is defined by

$$a_i = \sum_j w_{ij} o_j + \theta_i,$$

where w_{ij} is the *weight* assigned to the connection between the units i and j ($i \neq j$), $\theta_i = \bar{\theta}_i + I_i$ (I_i total “external” input to unit i , $\bar{\theta}_i$ fixed bias) and o_j represents the *output* coming from unit j . The output function is taken to be

$$o_j = \sigma(a_j) = \frac{1}{1 + e^{-a_j}}.$$

Note that the transfer σ -functions are a standard way to describe a “smooth” switch. While the sigma function in the original paper by Pasemann can take values between 0.5 and 1 for $a_j > 0$, we chose an alternative formulation (see equation 1).

In formulating our model we were inspired by these models presented in [21, 22], but contrary to Pasemann’s assumptions we considered neural *clusters* instead of single neurons, assuming that neurons in the same cluster fire at the same time. We also did not take any bias into account and we considered a random external input I and a more general σ -function

$$\sigma(a_j) = \frac{1}{1 + \exp[m(-a_j + q)]}. \quad (1)$$

For positive a_j our neuronal excitation model can vary between $\frac{1}{1 + \exp[m(-a_j + q)]}$ and 1; so one can adjust the value of q in order to move the lower bound that was set to 0.5 in Pasemann’s original formulation [21, 22]. Our model consists of the four units (neural clusters) described above, which interact as described in Figure 6. It is stressed that little is known about these connections. Therefore, on one hand it is difficult to realistically estimate the parameters, but on the other, the model has the potential of giving a greater insight into the understanding of the system.

Having no specific data to inform the weight choice, the numbers associated to the various connections shown in Figure 6 are simply the times (over four experiments) in which the corresponding behavioural transition is observed; then the considered weights will be these numbers divided by four. In this way, it is implicitly assumed that each behavioural switch is proportional to the weight of the corresponding connection. However, this assumption is just taken as a starting point to associate numbers to the weights, and further work will be carried out to have better estimates of the model parameters.

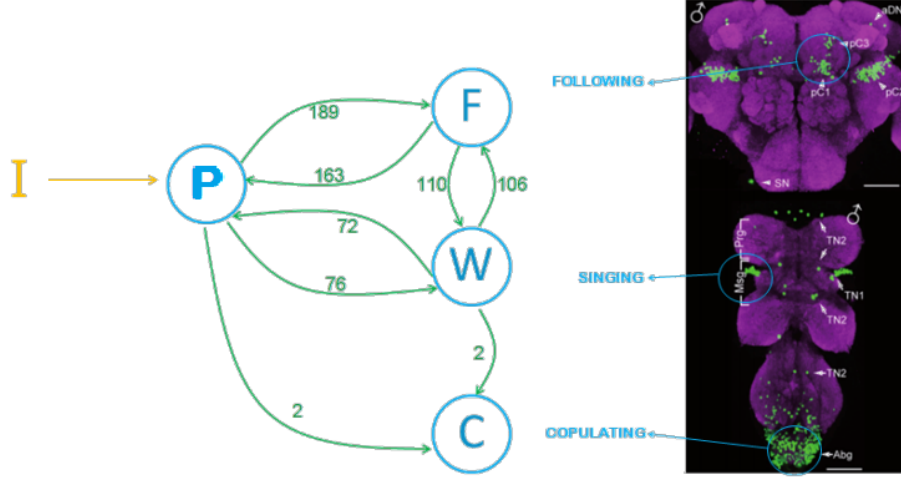


Figure 6: Schematic view of the model, compared with an image of neurons expressing the sex-determining gene *doublesex* in the *Drosophila* brain and ventral nerve cord. The *doublesex* gene is necessary and sufficient for flies displaying male courtship behaviours [10]. The fly brain was prepared and imaged by Hania Pavlou, who co-authors this paper. In the image, *doublesex* expressing neurons express a green fluorescent protein (GFP) while immunostaining of neuropils gives the magenta background. In the schematic view of the model the numbers on the edges are the number of times the corresponding behavioural switch is observed in four experiments.

In writing the equations describing the activity of each cluster, it is assumed that the clusters F and W reciprocally reduce the output coming from the processing unit P , and this output is also reduced by the activity of C . More precisely, being F_n the activation of the cluster F at time n , the value of F_{n+1} is given by $w_{PF}\sigma(P_n) \cdot \sigma(F_n - W_n - C_n) + w_{WF}\sigma(W_n)$, where the second term is due to the connection from W to F , shown in the diagram, and the former term takes into account the connection from P to F “reduced” by the activity of the clusters W and C . This approach will hopefully take into account a sort of “hierarchy” among the neural clusters: it is observed that for example copulation is “stronger” than following and wing extension, so we hope to see a kind of ordered sequence in the behaviours emerging from this neural activity.

Applying similar reasoning for all the four units, the equations describing the network are

$$P_{n+1} = I_n + w_{FP}\sigma(F_n) + w_{WP}\sigma(W_n) \quad (2)$$

$$F_{n+1} = [w_{PF}\sigma(F_n - W_n - C_n)] \cdot \sigma(P_n) + w_{WF}\sigma(W_n) \quad (3)$$

$$W_{n+1} = [w_{PW}\sigma(-F_n + W_n - C_n)] \cdot \sigma(P_n) + w_{FW}\sigma(F_n) \quad (4)$$

$$C_{n+1} = [w_{PC}\sigma(F_n + W_n)] \cdot \sigma(P_n) + w_{WC}\sigma(W_n), \quad (5)$$

where I_n denotes the external stimulus at time n and σ is the one defined in (1). Note that I_n here depends on the female response at time n and, in a first instance, we will take it to be random.

A first numerical simulation of the model (performed in MATLAB) can be

appreciated in Figure 7 where the neuronal activity of the different clusters is plotted for about 60 time steps.

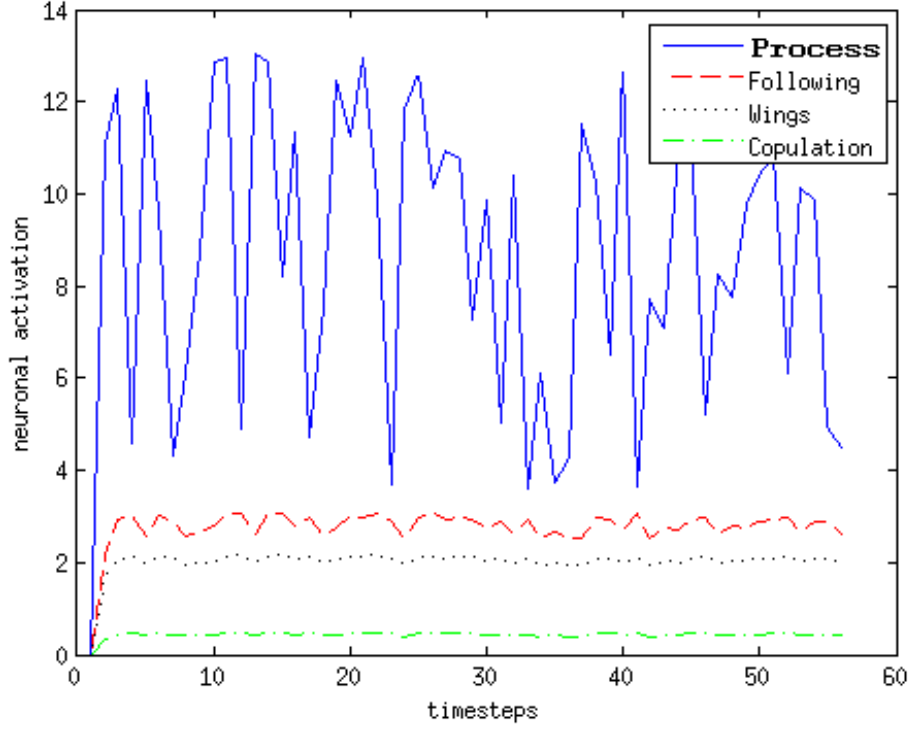


Figure 7: Simulation of neural activity of the four neural clusters. Here, the following parameter values were used: $w_{BF} = 0.01 \times 47.25$, $w_{FB} = 0.01 \times 40.75$, $w_{BW} = 0.01 \times 19$, $w_{WB} = 0.01 \times 18$, $w_{BC} = 0.1 \times 0.5$, $w_{FW} = 0.01 \times 27.5$, $w_{WF} = 0.01 \times 26.5$, $w_{WC} = 0.1 \times 0.5$, $m = 0.1$ and $q = 0$. The weights were multiplied by a constant for the clarity of the figure (for the same reason, all the equations were multiplied by the factor 10). Also, it seems reasonable to consider bigger values for w_{BC} and w_{WC} than the averages coming from the experiments, because these values look too small to be realistic. Concerning m and q , we have no information about them and further parameter estimation is needed to inform their values more precisely.

The simulation shows that in this case the system very quickly reaches a “quasi-equilibrium”, having the different cluster activities oscillating around a fixed value.

To convert these results into behavioural output (which would then be comparable with real data), it then assumed that a certain behaviour is displayed by the fly when the activation of the corresponding neural unit is above a certain threshold. Therefore, Figure 8 shows the “translation” of the dynamics shown in Figure 7: here we have a pattern of the same form of the available behavioural data.

Although it is still too early to decide whether this output is “good” or not, this preliminary result shows that this neural approach might be a good way to study the model. In fact, it produces an output which is comparable with the

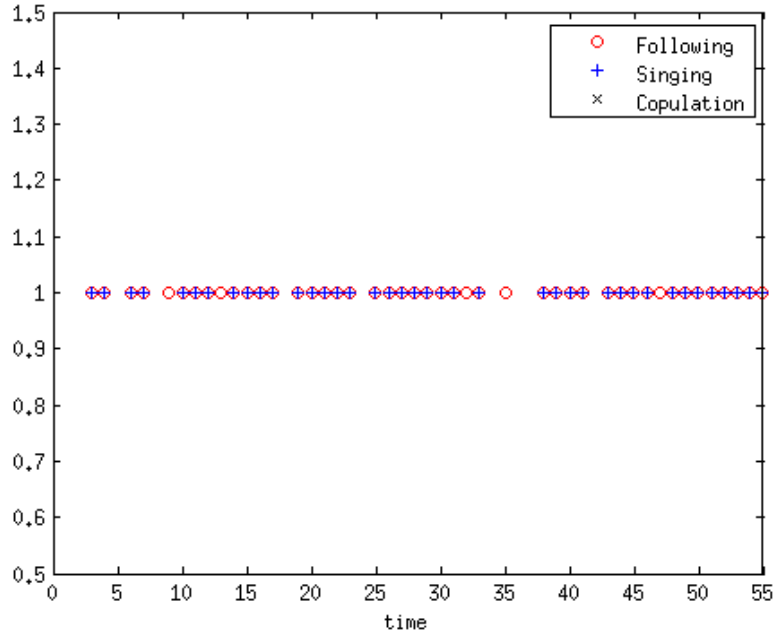


Figure 8: Behavioural pattern emerging from the previous simulation of neural activation. Here the thresholds are taken as follows: $\theta_F = 2.6$, $\theta_W = 2$ and $\theta_C = 3$ (we assumed $\theta_C > \theta_W$ because it seems reasonable to require higher excitation for copulation).

experiments, and the general shape of the network is based on widely accepted biological knowledge.

The main aspect of this model that can be largely improved is the parameter estimation. The neural activation presently considered does not correspond to a precisely defined physical quantity, and it seems difficult to practically implement an experiment measuring the weights of connections between clusters. However, the data contained in the ethograms can be used to estimate the weights and the thresholds in the normal case. Then, if the model results fit the biological observations, this system could be used to speculate about the most relevant connections between neurons. This would have a big impact in studying the underlying mechanisms of impaired neural activity as the one observed in Parkinson’s disease.

4.2.2 Other Mathematical Models of Neurons and Simple Networks

In 1943, McCulloch and Pitts [23] devised a simple mathematical model of a neuron which subsequently led to the development of the field of Artificial Neural Networks (ANNs), see [24] for an introduction to ANNs. The artificial neuron is made up of four basic components: an input vector, say x_j , a set of synaptic weights, say w_{ij} , a summing junction with an activation (transfer) function, say ϕ , and an output, usually denoted by y_i . The model describes a neuron acting

like a binary processing unit, where

$$y_i = \phi \left(\sum_j w_{ij} x_j \right)$$

and ϕ is usually a sigmoid function. Unfortunately, this simple binary model is not suitable for real biological neurons. In 1952, Alan Lloyd Hodgkin and Andrew Huxley were modelling the ionic mechanisms underlying the initiation and propagation of action potentials in the giant squid axon [25]. By treating each component of the excitable cell as an electrical element, and applying the conservation of electric charge on a piece of membrane, they were able to derive a set of Ordinary Differential Equations (ODEs) for membrane current density, see [24] for more information. The Hodgkin-Huxley (HH) ODEs have served as a classic reference in brain science and neurophysiology for several decades, unfortunately, these equations did not have a sound circuit theoretic foundation but were derived using empirical methods. In [26, 27], Chua et al. show that sodium and potassium ion-channel memristors are the key to generating the action potential in the HH ODEs, and that they are the key to resolving several unresolved anomalies associated with these ODEs.

Many mathematical neuronal models have been developed since the publication of the HH paper, simplified models directly relevant to this project are highlighted here. In 1961 and 1962, Fitzhugh [28] and Nagumo [29], respectively, derived a set of ODEs (essentially a reduction of the HH ODEs) to model the activation and deactivation dynamics of a spiking neuron. The describing Fitzhugh-Nagumo (FN) ODEs are:

$$\frac{dv}{dt} = c \left(v - \frac{v^3}{3} + w + I \right), \quad \frac{dw}{dt} = \frac{1}{c} (a - v - bw), \quad (6)$$

where v is a fast variable (in biological terms - the action potential), w represents a slow variable (biologically - the sodium gating variable), and I is the magnitude of stimulus current. The parameters a , b and c dictate the threshold, oscillatory frequency and the location of the critical points for v and w . A neuron will begin to oscillate when the input current I is above a critical threshold I_T , say.

A spiking-bursting ODE model of a neuron was introduced by Hindmarsh and Rose [30] in 1984, the three-dimensional system of ODEs has the form

$$\frac{dx}{dt} = y + f(x) - z + I, \quad \frac{dy}{dt} = g(x) - y, \quad \frac{dz}{dt} = r [s(x - x_R) - z], \quad (7)$$

where $f(x) = -ax^3 + bx^2$, and $g(x) = c - dx^2$, x is the membrane potential, y represents the transport of sodium and potassium through fast ion channels, and z is the transport of other ions through slow channels, x, y, z are dimensionless quantities here. The choices of parameters r and s make the model exhibit bursting, chaotic bursting and post-inhibitory rebound. The parameter x_R is the x -ordinate of the stable threshold critical point in the case where there is no external current applied. This simple model allows a good qualitative description of many different patterns of experimentally observed action potentials.

Arguably, the best simplified model to demonstrate most of the neuronal dynamics displayed experimentally is that devised by Izhikevich [31] in 2003,

although the model is biophysically meaningless. The ODEs are given by

$$\frac{dv_1}{dt} = 0.04v_1^2 + 5v_1 + 140 - v_2 + I, \quad \frac{dv_2}{dt} = \alpha(\beta v_1 - v_2), \quad (8)$$

with the auxiliary after-spike resetting

$$\text{if } v_1 \geq 30\text{mV, then } \begin{cases} v_1 \leftarrow c \\ v_2 \leftarrow v_2 + d. \end{cases} \quad (9)$$

The variable v_1 represents the membrane potential, v_2 is a membrane recovery variable, α describes the time scale of the recovery variable v_2 , β determines the resting potential of the neuron, and other parameters in (8) were chosen so that outputs aligned with human neurons. When the spike reaches 30 mV, the membrane voltage and the recovery variable are reset according to (9). In 2004, Izhikevich [32] compared the biological plausibility and computational efficiency of the following mathematical models: the HH model [25], the FN model [28, 29], the HR model [30], the Morris-Lecar (ML) model [33] and the spiking model of Izhikevich [31]. The HH and ML models are biophysically relevant, however, highly connected networks of these modelled neurons are computationally inefficient. The Izhikevich model is the computationally most efficient model capable of computing hundreds of thousands of interconnected neurons, however, they are biophysically meaningless.

We have carried out preliminary investigations for the simplest and most meaningful ODE model listed above, namely the FN ODE model (6). *Drosophila melanogaster* has different classes of neurons with different properties. We decided to reduce our study of neuron features on neuronal thresholds, as neuronal excitation is known to drive switches between courtship behaviours [16]. Different neural thresholds of each courtship behaviour are one possibility to explain this observation.

By changing the parameter c in the ODEs (6) we can alter the threshold of the neuron. For example, when $c = 3$ the threshold is approximately 0.4mV, and the amplitude of oscillation is approximately 2 units (see Figure 9), and when $c = 1$, the threshold is approximately 0.8mV, and the amplitude is approximately 0.5 units. Figure 9(a) shows that the threshold of the neuron is

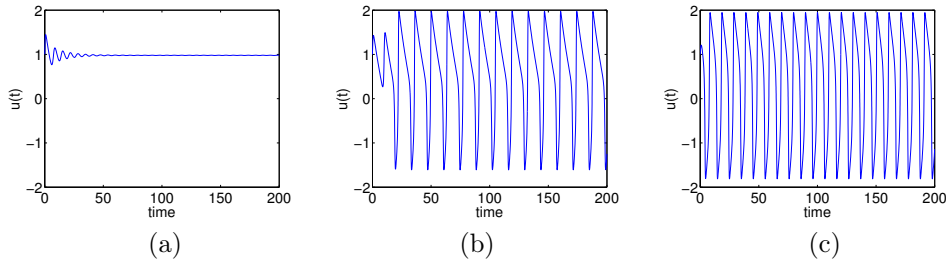


Figure 9: (a) Consider system (6), when the input is $I = 0.38\text{mV}$, the neuron does not fire; (b) when the input is $I = 0.4\text{mV}$, threshold is achieved and the neuron starts spiking; (c) as the input increases to $I = 0.5\text{mV}$, the frequency of firing increases.

not reached and hence it does not fire, when the input exceeds $I \approx 0.4\text{mV}$, the

neuron starts to fire with a frequency of about 0.073kHz, and when $I \approx 0.6$, the frequency has risen to approximately 0.098kHz. Figure 10 shows how the

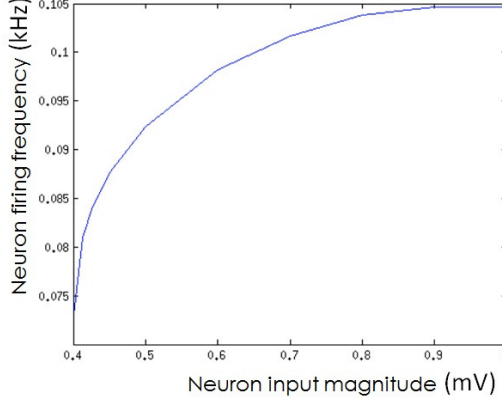


Figure 10: Graph of neuron firing frequency with respect to neuron input magnitude.

neuron firing frequency changes with respect to neuron input magnitude. Note that, with the FN model, as the input increases beyond $I \approx 1\text{mV}$, the frequency starts to drop again and eventually the solution jumps to the other stable critical point and the neuron ceases firing once more. Physically, once the threshold is attained the neuron will continue to fire at an increasing frequency up to some physical limit. Thus, using the FN ODE model it is possible to have neurons with different thresholds and having different firing frequencies. Next we want to model how the neurons, and eventually the neuron clusters, are connected. As a simple starting point we will consider linearly coupled FN models as depicted in system 10

$$\begin{aligned} \frac{dv_1}{dt} &= c \left(v_1 - \frac{v_1^3}{3} + w_1 + I + k \left(\frac{dv_2}{dt} - \frac{dv_1}{dt} \right) \right), & \frac{dw_1}{dt} &= \frac{1}{c} (a - v_1 - bw_1), \\ \frac{dv_2}{dt} &= c \left(v_2 - \frac{v_2^3}{3} + w_2 + I + k \left(\frac{dv_2}{dt} - \frac{dv_1}{dt} \right) \right), & \frac{dw_2}{dt} &= \frac{1}{c} (a - v_2 - bw_2), \end{aligned} \quad (10)$$

where k is a coupling coefficient.

A far more realistic nonlinear coupling between neurons is provided by transfer functions of the form

$$\sigma(x) = \frac{1}{1 + e^{m(\tau-x)}}, \quad (11)$$

where τ determines a threshold and m denotes the steepness of the curve.

In 2009, Borresen and Lynch [34] coupled HH ODEs together using a transfer function of the form (11) and demonstrated logical AND and OR operations of HH neurons. Three years later, these ideas were galvanized and an international patent was published [35]. The patent illustrates how it is possible to construct binary logic gates from coupled threshold oscillators connected using both excitatory and inhibitory connections. Figure 11 displays the schematics of the binary oscillator half-adder along with the corresponding time series of input/output. The simulations were run based on FN oscillators [36].

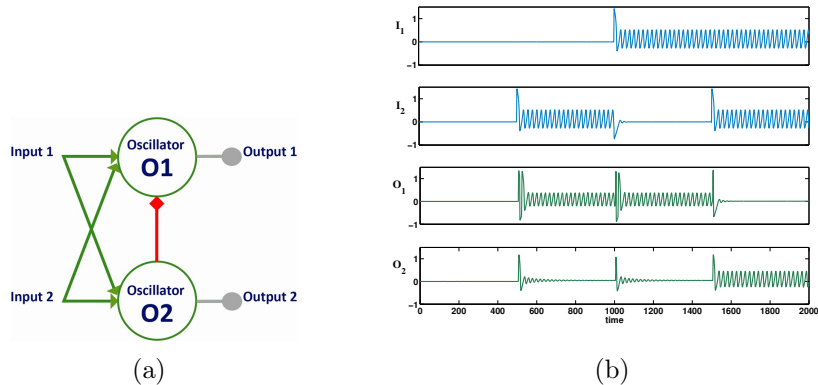


Figure 11: (a) Schematic of a binary oscillator half adder comprising two inputs I_1 and I_2 , two oscillators O_1 and O_2 and a set of excitatory synaptic connections with weights w_1, w_2 , and an inhibitory connection with weight x_1 . The sum oscillator O_1 will oscillate if either I_1 or I_2 are active. The carry oscillator O_2 will oscillate if both I_1 and I_2 are active. The inhibitory connection x_1 , from O_2 to O_1 suppresses oscillator O_1 if O_2 is active. (b) Time series showing that the half-adder is functioning correctly when the oscillations are simulated using Fitzhugh-Nagumo systems. Oscillations are equivalent to a binary one in these simulations and no oscillation is zero.

In future work we will also need to model using Delay Differential Equations (DDEs) since delays are inherently present in neuronal networks.

5 Workshop Outcome and Future Work

We have followed up our work in Cambridge with a meeting in Oxford. We met for five days between November 19th and November 23rd 2014. During this meeting we presented our work to mathematicians and fly biologists from Oxford. We have received helpful feedback on our work. Specifically, we were able to improve our Markovian courtship simulations and inform our neuronal models with up-to-date physiological knowledge of courtship neurons.

During the November meeting we were able to link our Markovian random-walk model with our Pasemann-like neuronal model. While the random-walk model allows for rapid simulations, the Pasemann-like model might allow insights of mechanistic nature. For example, we can address the question "What distinguishes a neuronal network giving rise to normal and impaired courtship?". In order to study this question we have recently contacted Daniel Segal who leads a group working on neurodegeneration in *Drosophila* [13]. Daniel Segal has welcomed our initiative to model courtship in flies and we have started a collaboration.

In addition we have started to work on techniques to quantify deviations from our models. As our model can be used as baseline, quantifying deviations from baseline is crucial to identify regions of interest for further research. We plan to publish a paper to disseminate our models and additional techniques we

have developed following the maths study group.

ACKNOWLEDGEMENTS

The authors acknowledge support from the NC3Rs and the POEMs network who have funded both the Mathematics Study Group in Cambridge and our follow-up meeting in Oxford.

References

- [1] Arthur, B.J. et al. (2013) *Multi-channel acoustic recording and automated analysis of Drosophila courtship songs*. BMC Biol. 11, 1–11.
- [2] Billeter, J.-C. et al. (2006) *Control of male sexual behavior in Drosophila by the sex determination pathway*. Curr. Biol. 16, 766–776.
- [3] Bastock, M. and Manning, A. (1955) *The Courtship of Drosophila melanogaster*. Behaviour 8, 85–111.
- [4] Bastock, M. (1956) *A Gene Mutation Which Changes a Behavior Pattern*. Evolution (N. Y). 10, 421–439.
- [5] Coen, P. et al. (2014) *Dynamic sensory cues shape song structure in Drosophila*. Nature DOI: 10.1038/nature13131.
- [6] Cobb, M. et al. (1985) *The structure of courtship in the Drosophila Melanogaster species sub-group*. Behaviour 95, 203–223.
- [7] Kohatsu, S. et al. (2011) *Female contact activates male-specific interneurons that trigger stereotypic courtship behavior in Drosophila*. Neuron 69, 498–508.
- [8] Markow, T.A. and Hanson, S.J. (1981) *Multivariate analysis of Drosophila courtship*. Proc. Natl. Acad. Sci. U. S. A. 78, 430–434.
- [9] Rideout, E.J. et al. (2010) *Control of sexual differentiation and behavior by the doublesex gene in Drosophila melanogaster*. Nat. Neurosci. 13, 458–466.
- [10] Pavlou, H.J. (2014) *Intersecting doublesex neurons underlying sexual behaviours in Drosophila melanogaster*. University of Oxford, U.K.
- [11] Chakravorty, S. et al. (2014) *Mutations of the Drosophila myosin regulatory light chain affect courtship song and reduce reproductive success*. PLoS One 9, e90077.
- [12] McBride, S.M.J. et al. (2005) *Pharmacological rescue of synaptic plasticity, courtship behavior, and mushroom body defects in a Drosophila model of fragile X syndrome*. Neuron 45, 753–764.
- [13] Shaltiel-Karyo, R. et al. (2012) *A novel, sensitive assay for behavioral defects in Parkinson’s disease model Drosophila*. Parkinsons. Dis. 2012, 1–6.
- [14] Berman, G.J. et al. (2014) *Mapping the stereotyped behaviour of freely moving fruit flies*. J. R. Soc. Interface, 11, 20140672.
- [15] Clyne, J.D. and Miesenböck, G. (2008) *Sex-specific control and tuning of the pattern generator for courtship song in Drosophila*. Cell 133, 354–363.

- [16] Pan, Y. et al. (2012) *Joint control of Drosophila male courtship behavior by motion cues and activation of male-specific P1 neurons*. Proc. Natl. Acad. Sci. U. S. A. 109, 10065–10070.
- [17] Pan, Y. et al. (2011) *Turning males on: activation of male courtship behavior in Drosophila melanogaster*. PLoS One 6, e21144.
- [18] Shirangi, T.R. et al. (2013) *Motor control of Drosophila courtship song*. Cell Rep. 5, 678–686.
- [19] Liepe, J. et al. (2014) *A framework for parameter estimation and model selection from experimental data in systems biology using approximate Bayesian computation*. Nat. Protoc. 9, 439–456.
- [20] Toni, T. et al. (2009) *Approximate Bayesian computation scheme for parameter inference and model selection in dynamical systems*. J. R. Soc. Interface 6, 187–202.
- [21] Pasemann, F. (1993) *Discrete Dynamics of Two Neuron Networks*. Open Systems & Information Dynamics 2(1) 49–66.
- [22] Pasemann, F. (1995) *Neuromodules: A dynamical systems approach to brain modelling*. Herrmann, H., Pöppel, E. & Wolf, D. (eds.) Supercomputing in Brain Research - From Tomography to Neural Networks 331–347.
- [23] McCulloch W. and Pitts W. (1943) *A logical calculus of the ideas immanent in nervous activity*, *Bulletin of Mathematical Biophysics*, **5**, 115–133.
- [24] Lynch S. (2014) *Dynamical Systems with Applications using MATLAB[®]* 2nd Edition, Springer International Publishing.
- [25] Hodgkin A.L. and Huxley A.F. (1952) *A qualitative description of membrane current and its application to conduction and excitation in nerve*, *J. Physiol.* **117**, 500–544, 1952. Reproduced in *Bull. Math. Biol.*, (1990) **52** 25–71.
- [26] Chua L.O., Sbitnev V. and Kim H. (2012) *Hodgkin-Huxley axon is made of memristors*, *Int. J. Bifurcation Chaos* **22** 1230011.
- [27] Chua L.O., Sbitnev V. and Kim H. (2012) *Neurons are poised near the edge of chaos*, *Int. J. Bifurcation Chaos* **22** 1250098.
- [28] Fitzhugh R. (1961) *Impulses and physiological states in theoretical models of nerve membranes*, *Biophys.* **1182** 445–466.
- [29] Nagumo J., Arimoto S. and Yoshizawa S. (1970) *An active pulse transmission line simulating 1214-nerve axons* Proc. IRL **50** 2061–2070.
- [30] Hindmarsh J.L. and Rose R.M. (1984) *A model of neuronal bursting using three coupled first order differential equations* Proc. R. Soc. London, Ser. B **221** 87102.
- [31] Izhikevich E.M. (2003) *Simple Model of Spiking Neurons*, *IEEE Transactions on Neural Networks* **14**(6) 1569–1572.

- [32] Izhikevich E.M. (2004) *Which model to use for cortical spiking neurons?* IEEE Transactions on Neural Networks **15**(5) 1063–1070.
- [33] Morris C. and Lecar H. (1981) *Voltage oscillations in the barnacle giant muscle fibre* Biophys. J. **35** 193–213.
- [34] Borresen J. and Lynch S. (2009) *Neuronal computers*, Nonlinear Anal. Theory, Meth. & Appl., **71** 2372–2376.
- [35] Lynch S. and Borresen J. (2012) *Binary Half Adder using Oscillators*, International Publication Number, WO 2012/001372 A1 1–57.
- [36] Borresen J. and Lynch S. (2012) *Oscillatory Threshold Logic*. PLoS ONE 7(11): e48498. doi:10.1371/journal.pone.0048498.